JOURNAL OF MATERIALS SCIENCE 28 (1993) 5486–5494

Silicon carbide platelet-reinforced silicon nitride composites

D. BARIL
Alcan International Limited, Arvida Research and Development Centre, 1955 Mellon Blvd., Jonquiere, Quebec, Canada G7S 4K8

S. P. TREMBLAY
C-Axis Technology Limited, 2538 Dubose Street, Jonquiere, Quebec, Canada G7S 4K9

M. FISET
Laval University, Mining and Metallurgical Department, Sainte-Foy, Quebec, Canada G1K 7P4

Different grades of high aspect ratio SiC platelets were used to reinforce Si_3N_4. Dispersion of additives (4 wt % Y_2O_3 and 3 wt % Al_2O_3) was achieved by ball milling in ethanol using alumina balls, while dispersion of platelets was done by ball milling using plastic balls. Consolidation of the composites was carried out by uniaxial hot pressing. A slight decrease in flexural strength was measured, while significant increases in elastic properties, fracture toughness and Weibull modulus were noted. Microstructure and crack-propagation studies as well as reinforcement mechanisms are presented.

1. Introduction

Ceramic materials offer a very interesting potential for structural applications, especially when high resistance at elevated temperatures is required. Silicon nitride displays the following characteristics: high hardness, high strength at room and elevated temperatures, fairly high fracture toughness, good thermal shock resistance, good resistance to oxidation and corrosion, favourable tribological behaviour, low friction and low density. These many interesting characteristics make silicon nitride one of the most promising advanced ceramic materials for structural applications, such as balls and ball bearings, cutting tools, gas turbines, rotor blades, stator vanes, piston caps, moving valves, cylinder liners, etc. [1–4].

Nevertheless, material uniformity, reproducibility, reliability and brittleness are still problems to be dealt with for any type of ceramic-based material. Mechanical properties of monolithic ceramics, especially the fracture toughness, can be significantly increased by adding a second phase. High-temperature mechanical properties such as flexural strength and creep resistance could also be improved with reinforcement-particle addition [5–8].

Efforts have been made to reinforce silicon nitride by the addition of whiskers. Whiskers, however, are difficult to disperse uniformly and the composites are hardly densified. To date, these characteristics are technical limitations to achieve fully the potential benefit of the whisker reinforcement. Independent of their chemical nature, whiskers are also considered potentially carcinogenic [9] and should be handled with care to avoid health-related problems.

Theoretical modellings have demonstrated that high aspect ratio platelets may be an effective, environmentally safe alternative to whiskers [8, 10, 11]. Platelet-reinforced composites are easier to densify [12–14] and they have a better oxidation and impact resistance [15] than whisker-reinforced composites. Platelets are free-flowing powders, easy to handle and to disperse in either a dry or wet state. High aspect ratio α-SiC platelets are now available in several sizes and grades. Publications provide detailed characterization of these SiC platelets [16–18].

Alumina [12, 18–21], mullite [14, 21], silicon nitride [21–26], sialon [21] and molybdenum disilicide [7] have been studied as matrix materials for platelet composites. Decrease in composite flexural strength and increase in composite fracture toughness is generally observed.

A manufacturing process and microstructure evaluation of silicon nitride composites reinforced by SiC platelets consolidated by means of uniaxial hot pressing are presented in this paper. Room-temperature mechanical properties results and reinforcement mechanisms are discussed.

2. Experimental procedure

2.1. Raw material

Silicon nitride equiaxed α particles (UBE Industries Inc., NY, USA, grade SN-E10) were selected as the matrix starting powder. Particle size ranges between 0.1 and 0.3 μm and the specific surface area is 10–12 m^2g^{-1}. The crystalline composition of the powder is $> 95\%$ α and $< 5\%$ β. The oxygen content is less than 2.0% and the carbon content is less than 0.2%. Any other impurity level is under 100 p.p.m. All these data were provided by the manufacturer.

0022–2461 © *1993 Chapman & Hall*

Like most of the nonoxide ceramics, silicon nitride is characterized by a strong covalent interatomic bond. These crystals resist mechanical deformation but have low intracrystalline diffusivity. Hence, pure Si_3N_4 crystals cannot be consolidated into a dense body without sintering aids [1, 3, 27, 28]. The application of mechanical pressure, such as hot uniaxial pressing and hot isostatic pressing further increases densification of the Si_3N_4-based body, and/or lowers the amount of sintering aids necessary to achieve the same densification.

MgO, Y_2O_3 and Al_2O_3 are the most common sintering aids with silicon nitride. They react with the SiO_2 layer at the surface of the Si_3N_4 powder to form an inter-particular molten silicate phase. The melt activates the following sintering mechanisms: particles rearrangement due to the capillarity force of the melt and dissolution of α grains; recrystallization of Si_3N_4 in β rod-like grains; and grain growth [27, 28]. Other sintering aids were also successfully employed [26].

When used as a sintering aid, magnesia produces a silicate melt that is more favourable to densification than alumina and yttria at comparable temperatures. However, while it facilitates the densification, it also reduces the high-temperature mechanical properties compared to alumina and yttria. A combination of 4 wt % yttria and 3 wt % alumina was found to be very effective as sintering aid where an ideal combination of room-temperature and high-temperature mechanical properties was observed [1]. This composition was then chosen as matrix material to study the influence of SiC platelet addition, even though high-temperature mechanical properties, often critical for ceramic-based composites, were not studied in this work because it could be a topic of further studies with this system.

Silicon carbide platelets were supplied by C-Axis Technology (AZ, USA) in three different grades: Super Fine (SF), Fine (F) and Medium (M). Scanning electron micrographs of SF and F grade platelets are presented in Fig. 1, showing plate-shaped particles of uniform size. The average particle size of SF, F and M grade platelets are, respectively, 11, 17 and 24 μm, all with a narrow size distribution. The maximum size of platelets is controlled to -37 μm for grade M by means of regular sieving and to -20 μm for grades F and SF by means of ultrasonic sieving. Platelets have an α crystalline structure and an aspect ratio of 8–10, irrespective of their grade. The impurity level of each element is < 0.01 wt %, except for aluminium (about 0.8 wt %) because platelets were acid washed by the supplier. The oxygen layer on the SiC surface is about 0.2 nm thick and the platelets contain virtually no free carbon. Details regarding surface characterization, X-ray diffraction analysis, transmission electron microscopy (TEM) observations, aspect ratio measurements, chemical analysis, etc., are described in other works [16–18].

2.2. Composite fabrication

Starting matrix powders, Si_3N_4, 4 wt % Y_2O_3 and 3 wt % Al_2O_3 were mixed with ethanol (about 50 wt %) to form a slurry whereby sintering additives could be uniformly dispersed by ball milling for about 10 h using alumina balls in an alumina container. Platelets were then added to the slurry in the desired proportion. Alumina balls were replaced by plastic balls to prevent breakage of platelets and the slurry was again ball-milled for 1 h to disperse the platelets within the matrix powder mixture.

The slurry was later evaporated and mechanical agitation was maintained to prevent platelets from settling, until the slurry was viscous enough to be left for complete drying. The dried cake of mixed powders was gently milled and screened to -212 μm to obtain free-flowing composite agglomerated powder, which is easier to handle. The composite powder was then hot pressed at 1750 °C for 90 min under a 55 MPa pressure in a nitrogen atmosphere using a high-density graphite die. Hot pressings produced plates 40 mm × 48 mm × 10 mm thick or discs 30 mm diameter and 5 mm thick. The densities of the samples were measured using the Archimedes deionized water-immersion technique.

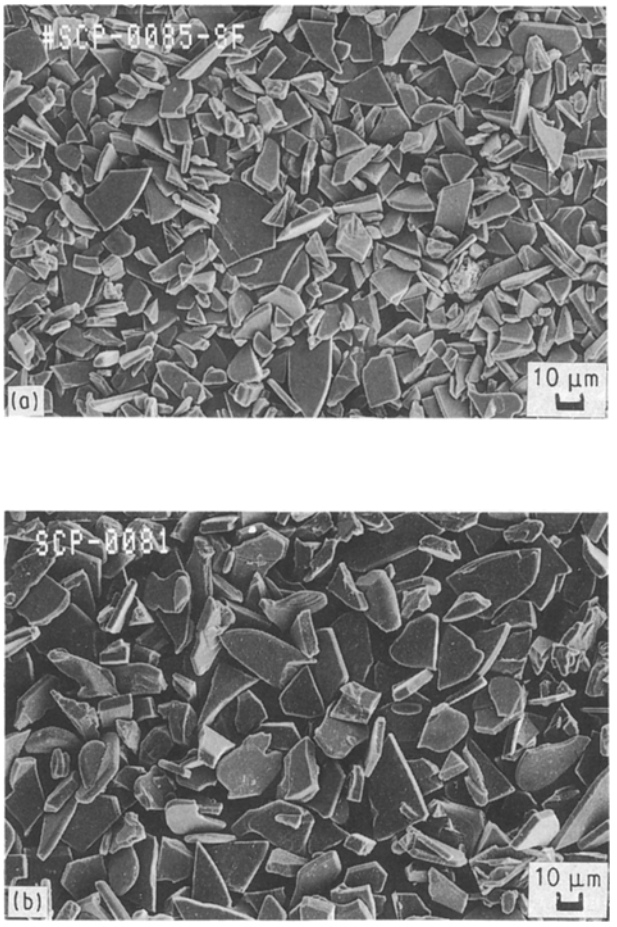

Figure 1 Scanning electron micrographs of (a) SF and (b) F grade SiC platelets.

2.3. Composite characterization

Observations using optical microscopy and SEM were carried out on polished and fracture surfaces of composites to observe their microstructure. Polished surfaces of some composites were dipped in molten NaOH at 350 °C for approximately 30 s to reveal

matrix grain size and shape, by dissolving the silicate intergranular phase. Artificial cracks were made by Vickers microindentations on unreinforced and reinforced Si_3N_4 polished surfaces to observe the effect of platelets on crack propagation.

Elastic properties were evaluated using ultrasonic velocity measurements in the as-machined condition on 3 mm × 3 mm × 4 mm pieces cut from tested chevron-notched samples. Measurements were made using the pulse-echo-overlap and pitch/catch technique. Ultran™ WC12-10 and SDB12-20 and KB-Aerotech™ Alpha 2 transducers were used to generate compressive and shear waves, at frequencies of 10, 20 and 15 MHz, respectively. An MP215 pulser, an MR101 receiver from Metrotek™ and 2236 oscilloscope from Tektronic™ completed the measuring system.

The geometry of the specimen and the experimental apparatus enabled the measurement of nine independent velocity values, V_{ij}, for each specimen. Indeed, one compression or L wave and two shear or T waves were considered in three orthogonal directions as shown in Fig. 2. The average value of three measurements taken at different positions along the length of the specimen for each velocity was used to evaluate the velocities in directions 2 and 3. Velocity measurements in direction 1 were made on samples 3 mm × 4 mm in length cut from one end of each specimen. In this particular direction only one measurement could be made for each ultrasonic wave.

The variation in ultrasonic velocities with the propagation directions in a specimen is too small to calculate the elastic constant with a good precision assuming a transversely isotropic material. We can therefore assume that silicon nitride with or without platelet reinforcement has an isotropic symmetry [29–31]. The formulae used to calculate the elastic constants (Young's modulus, E, and Coulomb modulus, G), assuming an isotropic material, are

$$E = (V_T)^2 \rho \frac{(3V_L^2 - 4V_T^2)}{(V_L^2 - V_T^2)} \quad (1)$$

$$G = (V_T)^2 \rho \quad (2)$$

where ρ is the bulk density, V_L and V_T are, respectively, the average longitudinal and transversal ultrasonic velocities. For linear elastic isotropic solids, E and G are sufficient to define elastic behaviour completely, giving interconnecting relations with other properties, e.g. Poisson's ratio.

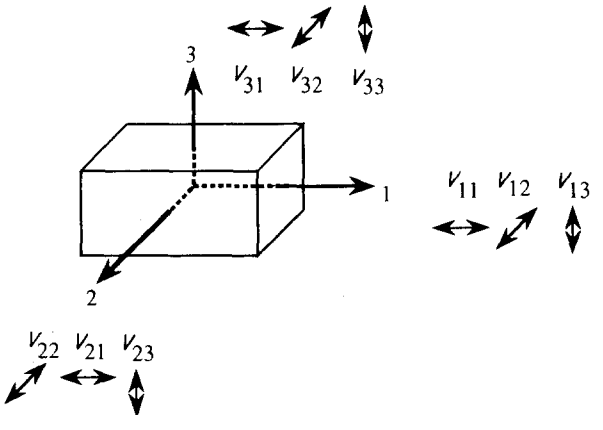

Figure 2 Velocity designation for ultrasonic waves.

Modulus of rupture (MOR) bars were machined from hot-pressed discs while chevron-notched samples were machined from hot-pressed plates. Every bend specimen was machined in order to angle the tensile surface perpendicular to the hot-pressing axis under tension. Flexural strength evaluation was carried out according to MIL STD 1942 [32] using specimen size A (1.5 mm × 2 mm × 25 mm) with a four-point bend fixture, which has an inside span of 10 mm and an outside span of 20 mm. The loading rate was 0.5 mm min^{-1} and about 15 MOR bars of each composition were tested. The geometric parameters of the chevron-notched samples are presented in Fig. 3. The four-point bend fixture used for fracture toughness evaluation had an outside span of 40 mm and an inside span of 20 mm. Six samples of each composition were tested to obtain a consistent average. Sample dimensions and a loading rate of 0.005 mm min^{-1} were selected to ensure slow crack growth within the chevron notch, essential for the validity of the results. Fracture toughness was calculated according to the slice model described by Munz *et al.* [33]. All these flexural tests were performed in air at room temperature. The Weibull modulus, which describes the flaw-size distribution (and thus the data scatter), was calculated according to the results of flexural strength [34].

Microhardness of the composites was measured using Vickers microindentation on polished parallel and perpendicular cross-sections. Each data point represents the average result of six indentations performed under a 20 kgf load. The load was applied for 5 s and the penetration speed was 125 μm s^{-1}.

3. Results and discussion

3.1. Microstructure evaluation

Optical microscopic observation revealed a uniform platelet distribution in the silicon nitride matrix irrespective of the grade of platelets. Fig. 4 presents typical photomicrographs of cross-sections parallel and perpendicular to the hot-pressing axis. No evidence of porosity can be detected in the pictures. Slight alignment of platelets perpendicular to the hot-pressing axis occurred during hot consolidation due to the viscous flow of the material.

Densification of every composite was always near 99.0% of the theoretical density (calculated according to the rule of mixtures). The theoretical density of the matrix is 3.27 g cm^{-3} [1] and that of the SiC platelets is 3.23 g cm^{-3} [16]. Platelet size and loading, at least up to 30 vol %, does not appear to affect the composite hot consolidation, as demonstrated in Fig. 5.

Vickers microindentations on unreinforced and 30 vol % SF grade composite, on a polished cross-section parallel to the hot-pressing axis, induced artificial cracks that reveal the effect of platelets on crack propagation. Fig. 6 presents low-magnification (× 170) backscattering electron mode scanning electron micrographs of indentations in these materials.

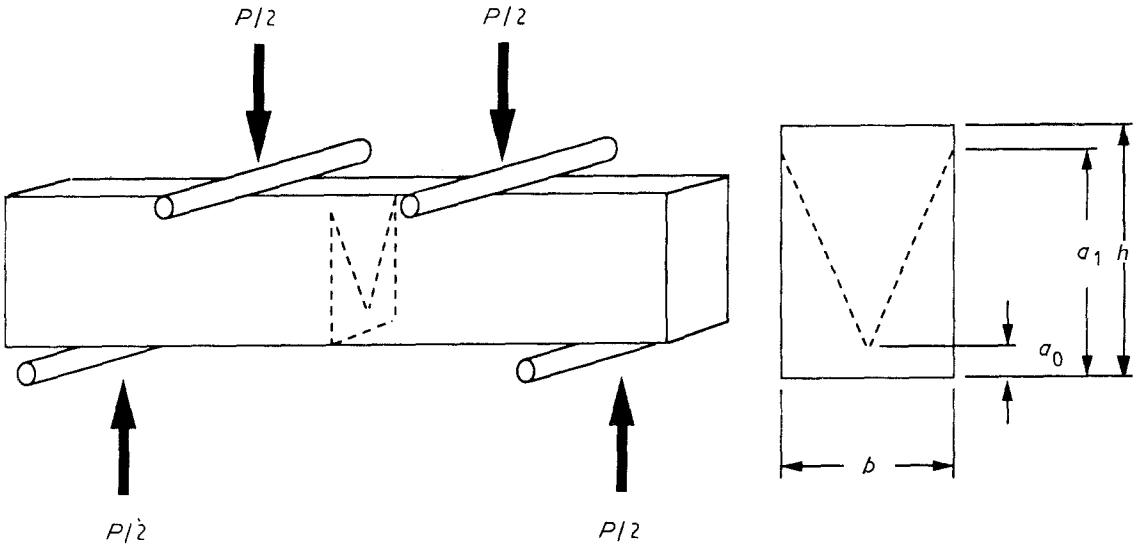

Geometric parameters: a_1 = 7 mm S_i = 20 mm
a_0 = 1 mm S_0 = 40 mm
b = 4 mm
h = 7 mm

Figure 3 Chevron-notched samples geometric parameters.

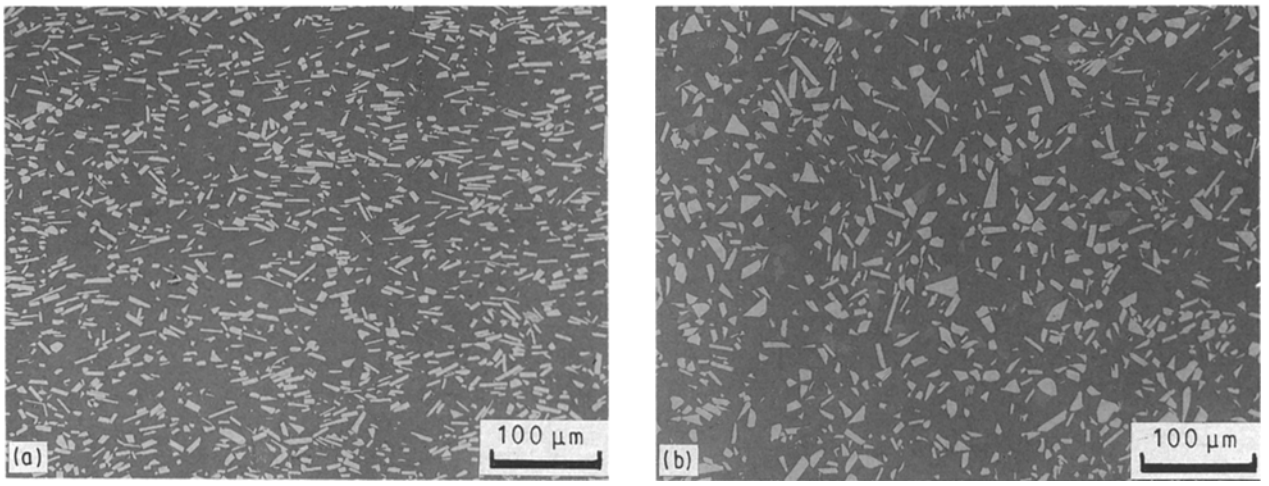

Figure 4 Photomicrographs of cross-sections (a) parallel and (b) perpendicular to the hot-pressing axis of 30 vol % SF grade composite. Evidence of platelet alignment perpendicular to hot-pressing axis can be observed.

Residual contact stress created a typical brittle material crack pattern surrounding the indentations. The crack length, however, is longer in the direction perpendicular to the hot-pressing axis than it is in the parallel direction, in both unreinforced and platelet-reinforced Si_3N_4. Therefore, anisotropic mechanical properties are expected for every composition, and the Si_3N_4 matrix intrinsically shows this characteristic. The machining orientation of MOR bars and chevron-notched samples should then be the most favourable to the evaluation of mechanical properties because the crack propagation direction is parallel to the hot-pressing axis.

Higher magnification scanning electron micrographs of crack propagation are presented in Figs 7–9. Relatively straight crack propagation, beginning at indentation corners, occurs in unreinforced Si_3N_4, while in the composite, even though in most cases cracks run through the platelets, the interference of platelets favours crack deflection, debonding and occasionally crack branching. Unlike unreinforced Si_3N_4, cracks are also initiated in the composite on the indentation side at platelet–matrix interfaces, as shown in Fig. 7. Therefore, platelet–matrix interfaces appear to have an effect on reinforcement mechanisms of composites.

Si_3N_4 matrix acicular grain shape, typical to β phase, between 1 and 3 μm in size can be clearly distinguished in Figs 8 and 9. X-ray diffraction (XRD) patterns confirmed the β crystalline structure of the

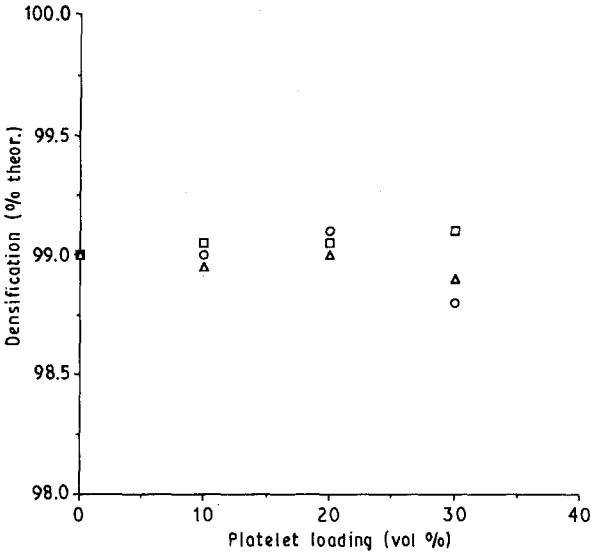

Figure 5 Influence of the platelet size and loading on the composite's hot consolidation. (□) SF, (○) F, (△) M.

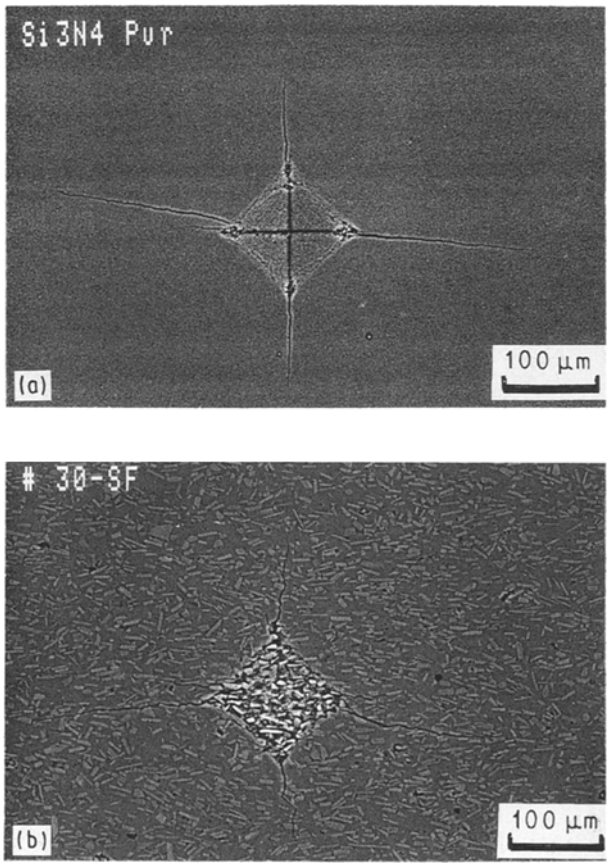

Figure 6 Scanning electron micrographs of microhardness indentations on (a) unreinforced and on (b) 30 vol % SF grade composite showing typical brittle material crack pattern but with an anisotropic mechanical behaviour.

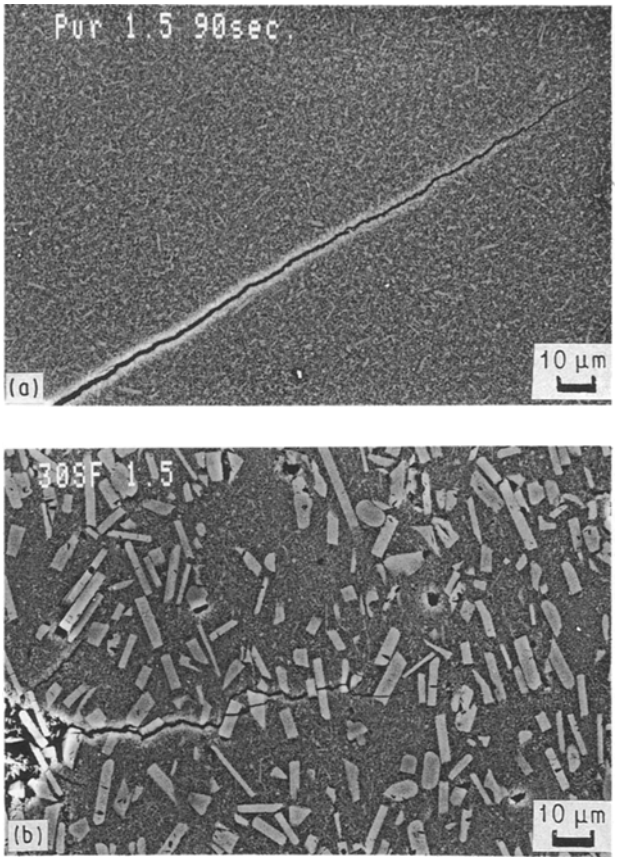

Figure 7 Platelet influence on crack initiation and on crack propagation in (a) unreinforced and on (b) 30 vol % SF grade composite.

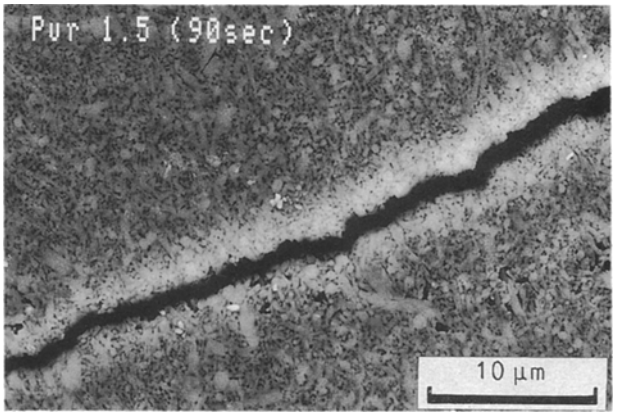

Figure 8 Matrix grains and crack propagation in unreinforced Si_3N_4 (polished surface chemically etched with molten NaOH).

Si_3N_4 matrix. Unreinforced Si_3N_4 shows slight crack deflection associated with the matrix intergranular nature of crack propagation (Fig. 8). No significant grain-growth modification seems to have occurred in composites during hot consolidation (Fig. 9). In the scanning electron micrographs of Fig. 9, grain alignment perpendicular to the hot-pressing axis (the crack propagation direction is parallel to the hot-pressing axis) similar to the platelet alignment is quite evident. The grain alignment that occurs during hot consolidation may explain the anisotropic behaviour of the Si_3N_4 matrix.

In Fig. 9, A–D highlight areas where reinforcement mechanisms act against crack propagation. Modulus load transfer can be observed near A, crack deflection near B, debonding near C and crack branching near D. Modulus load transfer from platelets to matrix reduces the constraint level on crack tips. This is also the case with crack branching, because it disperses the constraint level on to multiple crack tips. This reduction of the constraint level on crack tips hinders their

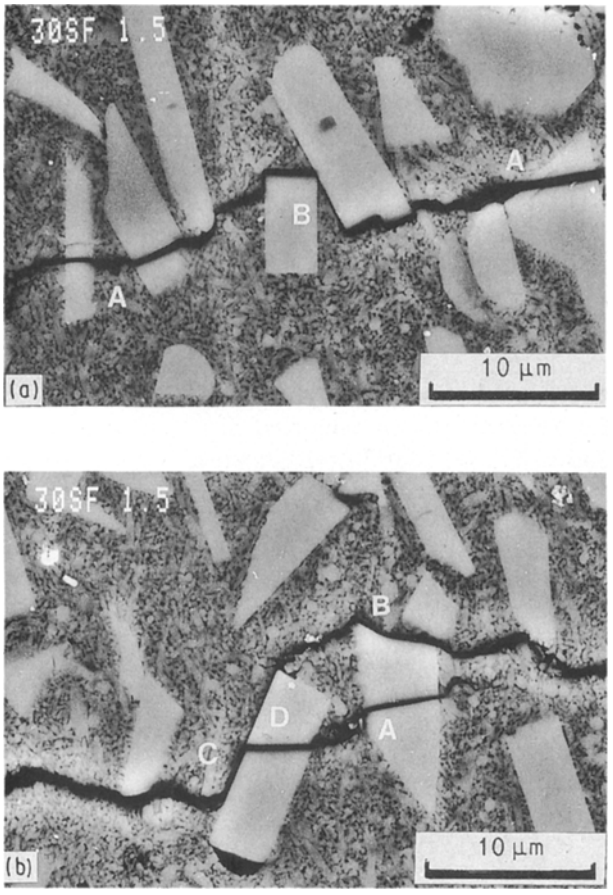

Figure 9 Matrix grains and crack propagation in 30 vol % SF grade composite (molten NaOH chemically etched, crack propagation along the hot-pressing direction) showing toughening mechanisms: (A) modulus load transfer; (B) crack deflection; (C) debonding; (D) crack branching.

TABLE I Literature elastic properties of α-SiC and β-Si_3N_4

	α-SiC	β-Si_3N_4
Modulus of elasticity (GPa)	410	317
CTE (10^{-6} °C^{-1})	5.2	3.2
Poisson's ratio	0.16	0.27

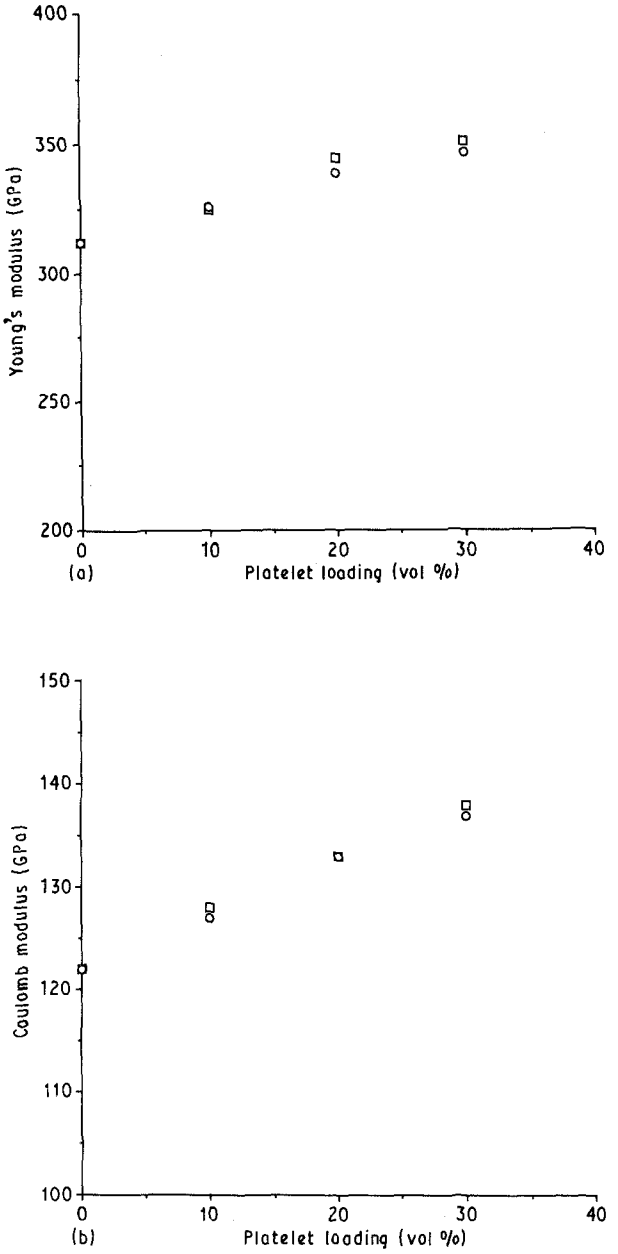

Figure 10 Ultrasonic evaluation results of elastic properties of the SiC_{pl}–Si_3N_4 composites: (a) Young's modulus; (b) Coulomb modulus. (□) SF, (○) F.

propagation and should contribute to the toughening of the composites. Crack deflection and debonding should also be favourable to the composite reinforcement by absorbing energy and by diverting away the direction of the crack propagation to the most favourable 90° orientation compared with the loading direction.

3.2. Elastic properties

Graphs of ultrasonic evaluation results are presented in Fig. 10. The Young's modulus augmentation is proportional to the addition of platelets and platelet size does not appear to influence its evolution (Fig. 10a). Data taken from articles available on elastic properties [31] of α-SiC and β-Si_3N_4, are presented in Table I. The Young's modulus evolution measured in this work follows rather precisely the rule of mixtures for these two compounds. This indicates that the modulus load transfer from platelets to the matrix is very effective, and that the interfacial bond between the platelets and the matrix is relatively strong.

The coefficient of thermal expansion (CTE) of the α-SiC is higher than the CTE of β-Si_3N_4. Therefore, during the cooling step following hot consolidation, SiC platelets tend to contract more than the Si_3N_4 matrix, but the strong chemical bond at the interface withstands the shear stress and holds them firmly together. Hence, at room temperature, SiC platelets are under tension while the Si_3N_4 matrix is under compression. The compression state of the Si_3N_4 matrix tends to cause cracks to close on themselves, especially near platelets. This hinders crack propagation in the matrix and enhances the contribution of the modulus load-transfer toughening mechanism to composite reinforcement. This mechanism is therefore considered to be predominant in this system.

Nevertheless, the thermal expansion mismatch between platelets and the matrix creates an important shear constraint at their interfaces. This may explain why crack deflection, debonding and crack branching are commonly found during crack-propagation observations.

According to these observations, the platelet–matrix interfacial strength, influenced by the sintering additives and to a lesser degree by the hot-consolidation conditions, should play a major role in composite-reinforcement mechanisms and may be the key factor in this system to obtain the desired combination of mechanical properties. The Coulomb modulus is also gradually improved with platelet addition (Fig. 10b).

3.3. Mechanical properties

Flexural strength results are plotted in Fig. 11. The addition of SF grade platelets does not significantly affect the flexural strength. It improves slightly up to 20 vol % loading (from 796 MPa for unreinforced Si_3N_4 to 808 MPa in the case of 20 vol % SF) and it slowly begins to decrease at 30 vol % loading (726 MPa). The addition of F grade platelets, however, progressively lowers the composite flexural strength with an increase in the loading of platelets, down to 630 MPa for 30 vol % loading.

The shear constraint that exists at the platelet–matrix interfaces, due to the thermal mismatch, increases when composites undergo external loading. These interfaces may therefore become crack initiation points that weaken composites and force platelets to act as strength-controlling defects.

The augmentation of platelet size has a greater effect on composite flexural strength because a large platelet has a wider interfacial area than a small platelet. Increased loading of platelets further decreases flexural strength because it increases the probability that a large platelet acts as a flaw. Hence, these flexural results appear to confirm that platelet–matrix interfacial strength is a critical factor in composite mechanical properties.

Fig. 12 presents plotted results of the Weibull modulus of the composite, which range from 11.5 for unreinforced Si_3N_4 up to 27.8 for 30 vol % SF grade composite. The scattered results of Weibull modulus are probably due to the relatively low number of samples tested. Still, this is a significant improvement of the Weibull modulus and an indication that the composites have a good mechanical properties reproducibility.

Fracture toughness progressively increases with the addition of platelets, as presented in Fig. 13, from 6.3 MPa $m^{1/2}$ for unreinforced Si_3N_4, to between 8 and 9 MPa $m^{1/2}$ for 30 vol % platelets with a typical standard deviation of 4%. This improvement confirms the contribution of the toughening mechanisms identified in earlier discussions. This improved tolerance of composites to flaws may also explain the Weibull

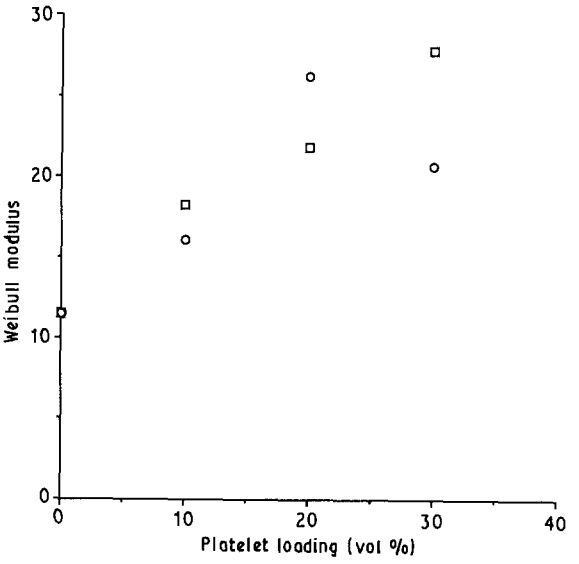

Figure 12 Weibull modulus of the SiC_{pl}–Si_3N_4 composites. (□) SF, (○) F.

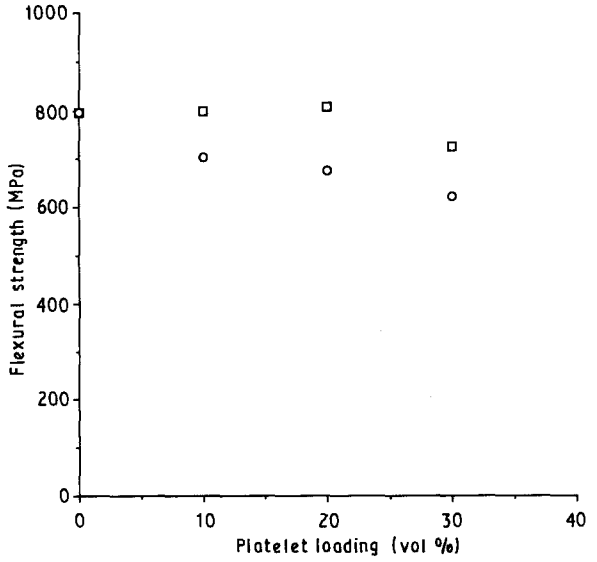

Figure 11 Flexural strength of the SiC_{pl}–Si_3N_4 composites. (□) SF, (○) F.

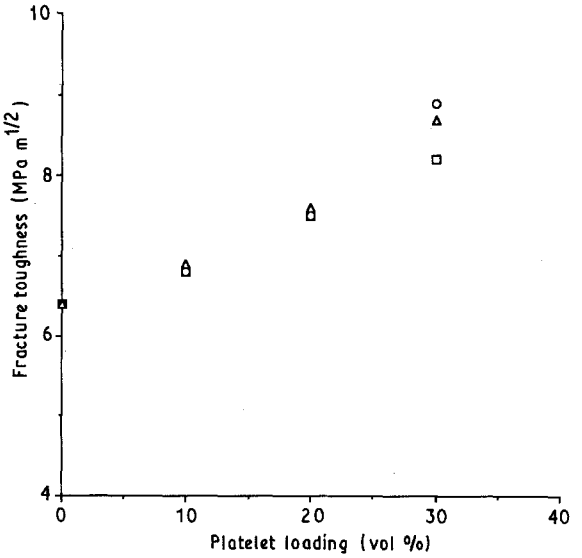

Figure 13 Fracture toughness of the SiC_{pl}–Si_3N_4 composites. (□) SF, (○) F, (△) M.

modulus increase, following the addition of platelets. Platelet size does not appear to affect composite toughening. It may be possible to increase fracture toughness further by reducing the interfacial bonding strength [21] mainly by using different compositions of sintering aids. This could promote toughening mechanisms such as crack deflection, debonding, crack branching and possibly pull-out of platelets.

Microhardness evaluation results are plotted in Fig. 14a. The addition of platelets does not significantly modify the hardness of the Si_3N_4. A slow increase of hardness can be observed with platelet loading, but this trend remains within the experimental error (typical standard deviation of 3%). No significant evolution was expected because Si_3N_4 and SiC both have approximately the same hardness [31]. SF grade platelets produce slightly better results than F grade platelets, which can probably be attributed to the strength of the material.

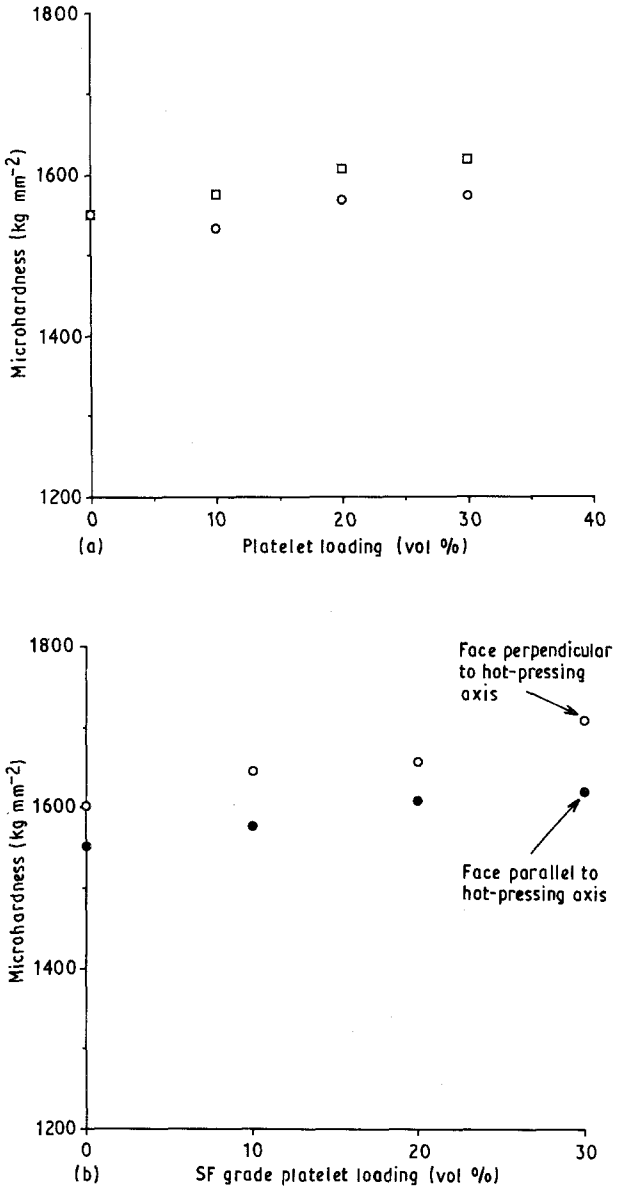

Figure 14 Vickers microhardness of the SiC_{pl}–Si_3N_4 composites. (a) Platelet-size influence; (b) surface-orientation influence. Platelet alignment contribution to anisotropic mechanical behaviour seems to be quite limited. (□) SF, (○) F.

The anisotropic nature of the Si_3N_4 matrix can once again be observed in Fig. 14b where the hardness differs according to surface orientation. The addition of platelets does not change the difference in hardness between the two surface orientations. Therefore, platelet alignment does not appear to have a bearing on the anisotropic mechanical properties of the composite.

4. Conclusion

Processing conditions produced near pore-free composites, regardless of platelet size and loading up to 30 vol %, with uniform platelet distribution and with some alignment perpendicular to the hot-pressing axis. The addition of 4 wt % yttria and 3 wt % alumina as sintering aids produced Si_3N_4 acicular 1–3 μm β matrix grains aligned perpendicular to the hot-pressing axis. Grain growth was unaffected by the addition of platelets. Even though both matrix grains and platelets were aligned, only the alignment of matrix grains has a significant effect on the material's anisotropic behaviour.

No significant modification of the composite flexural strength was observed with the addition of SF grade platelets, although a gradual decrease was observed with the addition of F grade platelets. Significant improvement in fracture toughness was obtained with the addition of platelets, irrespective of platelet size. An important increase of the composites' Weibull modulus, which is directly related to an increase in fracture toughness, was also obtained. The Young's modulus evolution with the addition of platelets followed the rule of mixtures of Si_3N_4 and SiC. Hence, the sintering aids used in this work produced strong platelet–matrix interfaces and favoured an effective load transfer. Modulus load transfer, enhanced by the thermal mismatch between SiC platelets and the Si_3N_4 matrix, was then identified as the predominant toughening mechanism, although crack deflection, debonding and crack branching also had an effect. Interfacial strength between platelets and the matrix is the key factor to obtain the desired combination of mechanical properties in this system.

In our case, the best combination of room-temperature mechanical properties was achieved with 30 vol % SF grade composite where a flexural strength of 726 MPa, a fracture toughness of 8.5 MPa $m^{1/2}$, a Weibull modulus of 28 and a Young's modulus of 350 GPa were obtained.

References

1. D. C. LARSON and J. W. ADAMS, AFWAL Contract Report, TR-63-4141 (1984) ITT Research Institute.
2. N. N. AULT, *Ceram. Bull.* **70** (1991) 882.
3. W. DWORAK and D. FINGERLE, *Brit. Ceram. Trans. J.* **86** (6) (1987) 170.
4. D. STEINMANN, cfi/Ber. DKG 67, no. 12 (1990) p. 584.
5. J. R. PORTER, F. F. LANGE and A. H. CHOKSHI, *Amer. Ceram. Soc. Bull.* **66** (1987) 343.
6. T. KANDORI, S. KOBAYASHI, S. WADA and O. KAMIGAITO, *J. Mater. Sci. Lett.* **6** (1987) 1356.
7. K. K. RICHARDSON, Report no. 3-56400/CT-002, IR and D Project no. 906M LTV Missiles and Electronics Group (1990).

8. N. CLAUSSEN, personnal communication, Technical University of Hamburg-Harburg, D-2100 Hamburg 90, Germany.
9. J. D. BIRCHALL, D. R. STANLEY, M. J. MOCKFORD, G. H. PIGOTT and P. J. PINTO, *J. Mater. Sci. Lett.* **7** (1988) 350.
10. M. R. PIGGOTT, in "Load-Bearing Fibre Composite" (Pergamon Press, Toronto, 1980) p. 42.
11. K. T. FABER and A. G. EVANS, *Acta Metall.* **31** (1983) 565.
12. J. G. KATZ, R. D. BLAKE and J. J. PETROVIC, *Ceram. Engng Sci. Proc.* **9** (1988) 725.
13. X. Y. ZHENG, F. P. ZENG, M. J. POMOROY and S. HAMPSHIRE, *Brit. Ceram. Proc.* **45** (1985) 187.
14. M. P. SEABRA, A. T. FONSECA, J. M. VIEIRA and J. L. BAPTISTA, Poster presented at the 7th Cimtec World Ceramics Congress, Montecatini, Italy, April 1990.
15. Y. AKIMUNE, *J. Mater. Sci.* **25** (1990) 3439.
16. C-Axis Technology, 14455 N. Hayden Road, Suite 228, Scottsdale, AZ 85260, USA, 1991.
17. S. G. MALGHAN, M. VAUDIN, J. P. CLINE, P.S. WANG, L.-S. H. LUM and M. K. JAIN, in "Proceedings of the Symposium on Composites: Processing, Microstructure, and Properties", held during the Second International Ceramic Science and Technology Congress, Orlando, FL, 12–15 November 1990, American Ceramic Society, Ohio, p. 253.
18. D. BARIL and M. K. JAIN, *Ceram. Engng Sci. Proc.* **12** (1991) 1175.
19. K. B. ALEXANDER, P. F. BECHER and S. B. WATERS, in "Proceedings of the XIIth International Congress for Electron Microscopy", San Francisco, USA (1990) p. 1032.
20. W. F. FISHER III, R. A. HABER, R. M. ANDERSON, in "Proceedings of the Symposium on Composites: Processing, Microstructure, and Properties", held during the Second International Ceramic Science and Technology Congress in Orlando, FL, 12–15 November 1990, American Ceramic Society, Ohio, p. 773.
21. H. SAKAI, K. MATSUHIRO and Y. FURUSE, *ibid.*, p. 765.
22. D. HOLZ, R. JANSSEN, K. FRIEDRICH and N. CLAUSSEN, *J. Eur. Ceram. Soc.* **5** (1989) 229.
23. N. CLAUSSEN, in "Proceedings of the 11th Risø International Symposium on Metallurgy and Materials Science: Structural Ceramics-Processing, Microstructure and Properties", Denmark, 1990 p. 1.
24. H. HANNINEN, R. A. HABER and D. E. NIESZ, in "Proceedings of the Symposium on Composites: Processing, Microstructure, and Properties", held during the Second International Ceramic Science and Technology Congress in Orlando, FL, 12–15 November 1990, American Ceramic Society, Ohio, p. 749.
25. S. M. KETCHION, G. LENG-WARD and M. H. LEWIS, *ibid.*, p. 757.
26. Y. FURUSE and K. MATSUHIRO, Eur. Pat. 90310090.7 (1990).
27. L. J. BOWEN, R. J. WESTON, T. G. CARRUTHERS and R. J. BROOK, *J. Mater. Sci.* **13** (1978) 341.
28. M. MITOMO, M. TSUTSUMI and H. TANAKA, *J. Amer. Ceram. Soc.* **73** (1990) 2441.
29. S. PELLETIER, PhD thesis, Laval University, Quebec, Canada (1991) p. 76.
30. J. A. GALLEGO-JUAREZ, in "Ultrasonic Methods in Evaluation of Inhomogeneous Materials" edited by A. Alippi and W. G. Mayer (Martinus Nijhoff, Erice, Italy, 1987) p. 281.
31. J. A. GALLEGO-JUAREZ, *ibid.*, p. 263.
32. MIL-STD-1942A, Department of the Army, Washington, DC.
33. D. MUNZ, R. T. BUBSEY and J. L. SHANNON Jr, *J. Amer. Ceram. Soc.* **63** (1980) 300.
34. D. W. RICHERDSON, in "Modern Ceramic Engineering" (Marcel Dekker, New York, 1982) p. 316.

Received 12 December 1991
and accepted 2 September 1992